Impacts of Cloud-Radiation-Circulation Interaction (CRCI) on Organized Convection and Extreme Precipitation

William K. M. Lau[1], Kyu-Myong Kim[2],

Jiun-Dar Chern[3], and W. K. Tao[4]

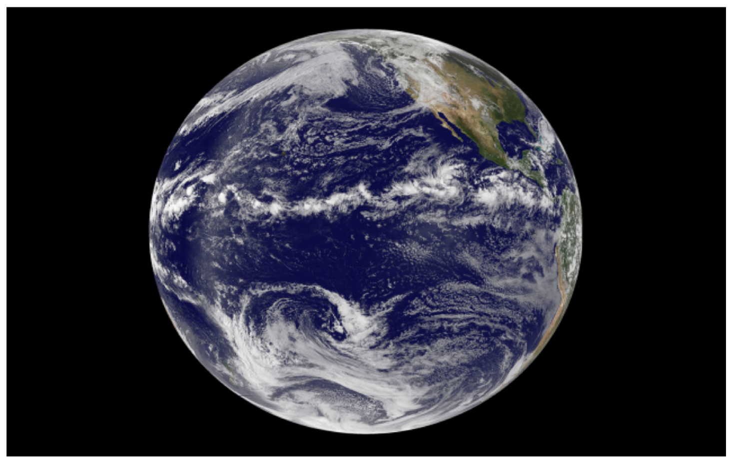

The ITCZ climate sub-system

[1] ESSIC, University of Maryland

[2] NASA/GSFC

The Deep Tropical Squeeze (DTS)

Under 2x or 4xCO_2, all 33 CMIP5 models showed a warmer and "moister" (increased specific humidity) world :

- Narrowing and intensification of the ITCZ convective core
- More high clouds in the deep tropics, less clouds in subtropics
- A deeper Hadley Circulation (HC), coupled to a widening subtropics
- Increased subsidence and low level moisture divergence in subtropics,
- Increased tropospheric, and near surface drying in a widening subtropics

(Lau et al., 2013 GRL, Lau and Kim, 2015, PNAS Wodzicki and Raap, 2016, Bryne and Schneider, 2016, Su et al., 2017.....)

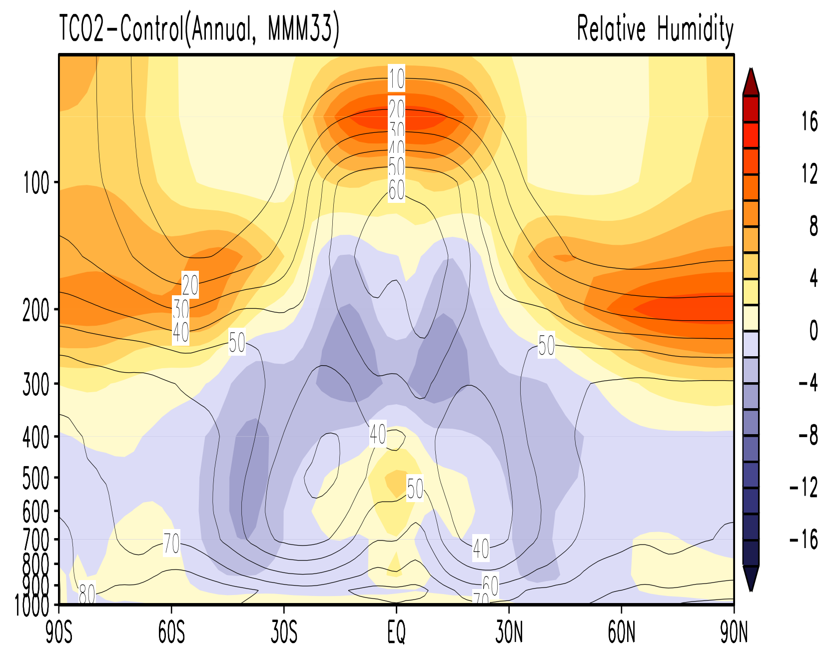

Thermodynamics:

$\delta R_h = \delta q / q_s - \alpha R_h \delta T$ CC *relationship*, $\alpha = L(R_v T^2)^{-1} \sim 6.5\% K^{-1}$

Dynamics:

Subsiding motion transports drier air from above

The Goddard Multiscale Modeling Framework (GMMF)

- The GMMF uses GEOS model as a host GCM and a 2D GCE model as the embedded CRM component.
- The moist parameterizations in GEOS GCM were replaced by a embedded 2D GCE at each GCM grid column to explicit simulate clouds and convections.
- The GEOS GCM has 2.0º X 2.5º grid spacing with 48 vertical layers stretching from the surface to 0.4 hPa.
- The 2D GCE has 32 x 44 (x-z) grid points with 4 km horizontal resolution and time step of 10 second.
- Globally there are more than 13,100 copies of 2D GCE running concurrently.
- The GMMF allows two-way interactions between cloud and large scale.

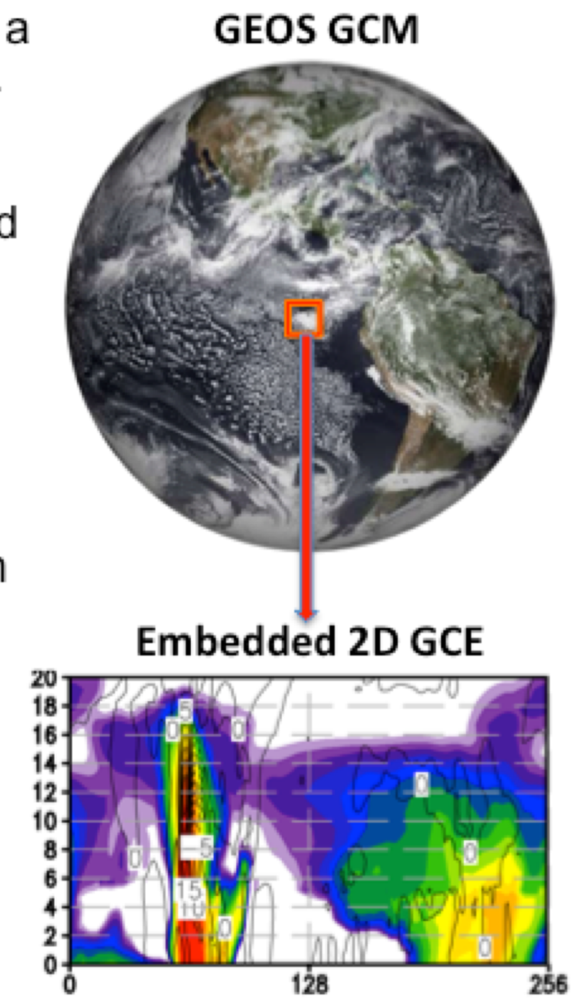

Cloud-radiation-circulation interactions : GMMF results

Sharpening
of ITCZ convection

More warming in tropics
More cooling in polar regions

Enhanced
mid-latitude
Strom tracks

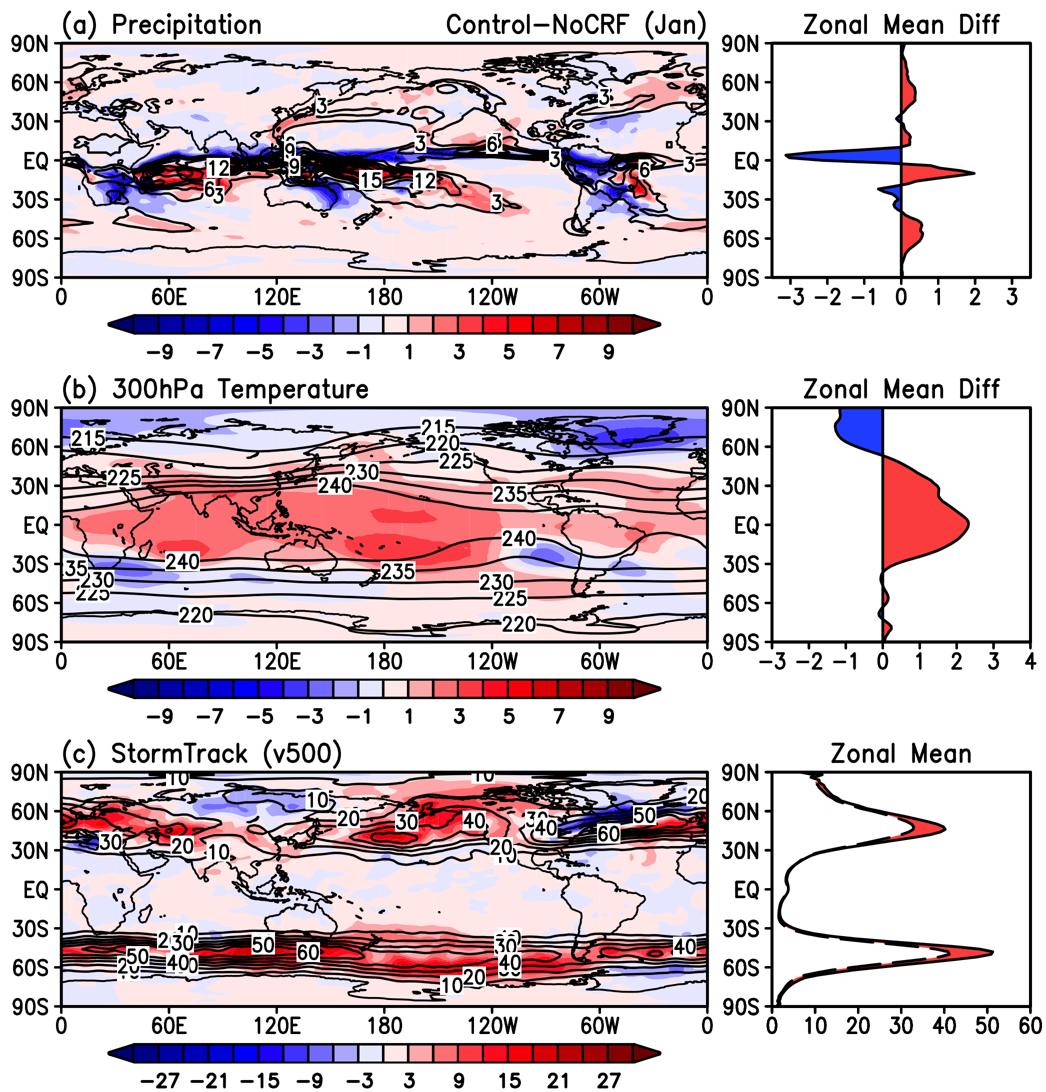

Changes in diabatic heating and dynamical tendencies

$$\frac{\partial \bar{s}}{\partial t} + \bar{\boldsymbol{v}} \cdot \nabla \bar{s} + \bar{\omega} \frac{\partial \bar{s}}{\partial p} = Q_R + L(c - e) - \nabla \cdot \overline{s' v'} - \frac{\partial \overline{s' \omega'}}{\partial p}$$

$$\frac{\partial s}{\partial t} = DYN + Q_{MP} + Q_{SW} + Q_{LW} + Q_{Res} \sim 0, \qquad for\ steady\ state$$

where s= dry static energy (CpT + gz)

$$DYN = -\left(\bar{\boldsymbol{v}} \cdot \nabla \bar{s} + \bar{\omega} \frac{\partial \bar{s}}{\partial p}\right)$$, dynamical tendency

Q_{MP}, heating by moist physics

Q_{SW}, shortwave heating

Q_{LW}, longwave heating

Q_{res} transients, unresolved subgrid processes

Diabatic heat balance in Control Climatology in GMMF: January

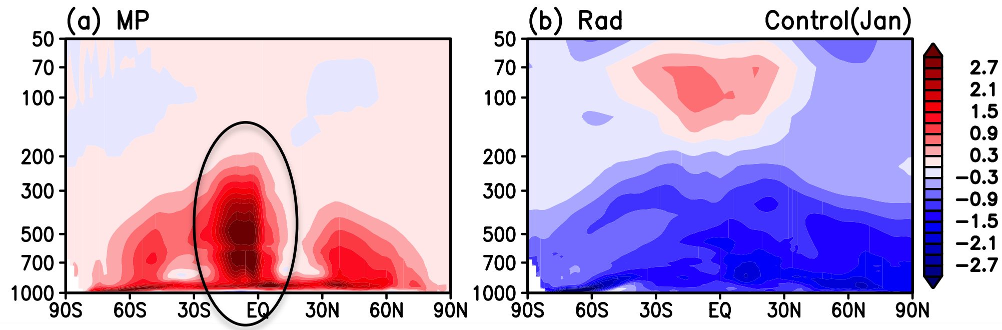

Radiative cooling

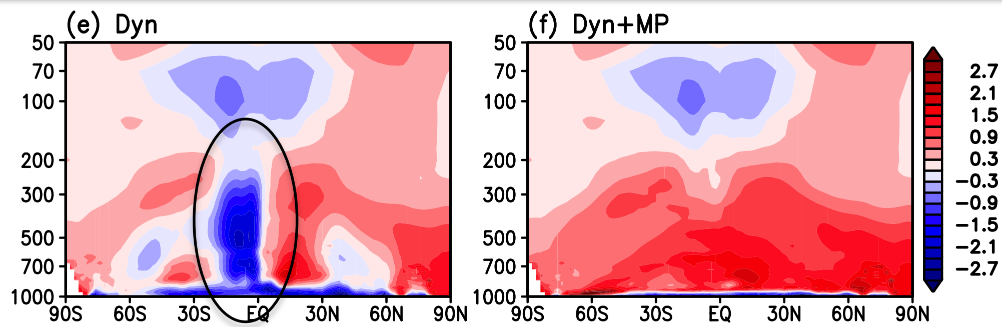

Weak temperature gradient in the tropic,
$w\,\Gamma_e \approx Q_{MP}/C_p$

Heat transport by dynamics

Dynamical adjustment induced by CRCI: Control minus No-CRF

DTS signal
in latent
heating

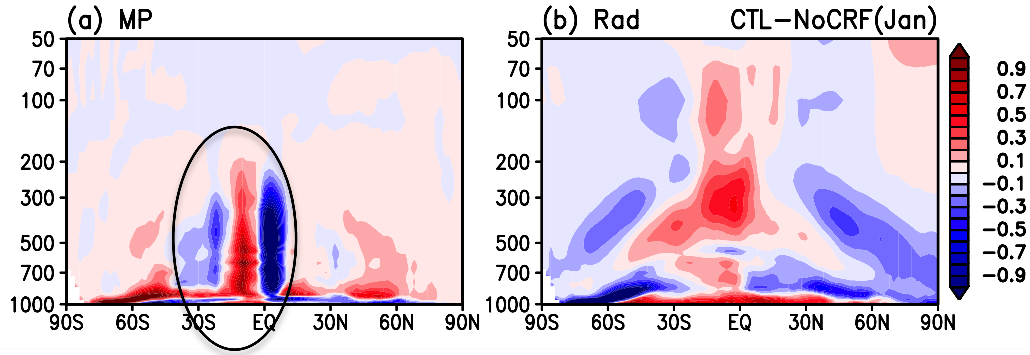

More radiative
warming in tropics
cooling in extratropics

LH ~ adiabatic
heating/cooling

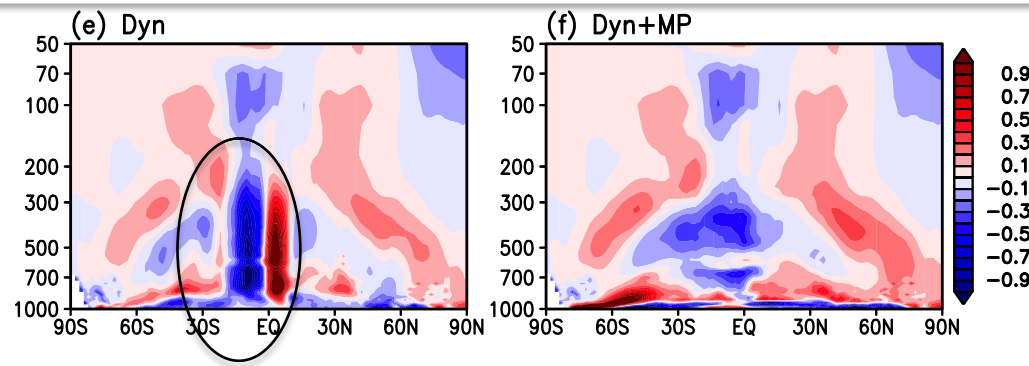

More poleward
heat transport

CRCI and extreme precipitation in the tropics (30S-30N)

wet gets wetter
dry gets drier

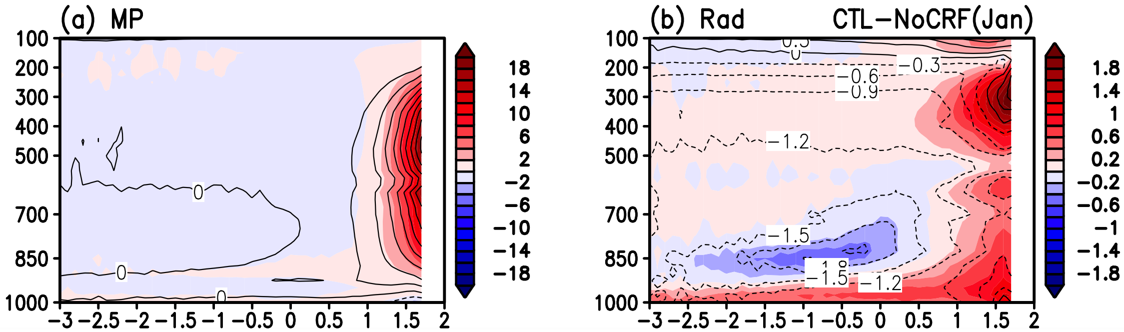

Radiation feedback;
wetter gets warmer,
drier gets cooler

$w\,\Gamma_e \approx Q_{MP}/C_p$
in heavy rain regions

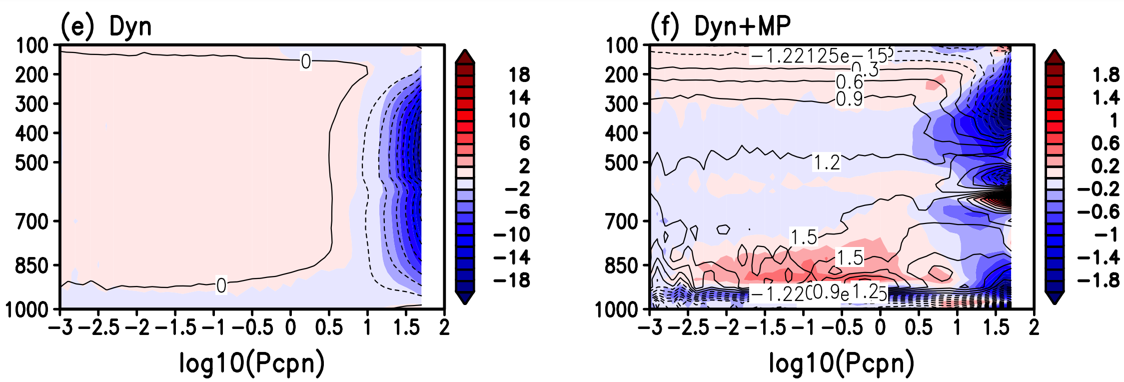

strong dynamic
cooling (warming)
In wet (dry) regions

← Drier Wetter→

← Drier Wetter→

Does CRCI modulate ITCZ Convection and Atmospheric Rivers?

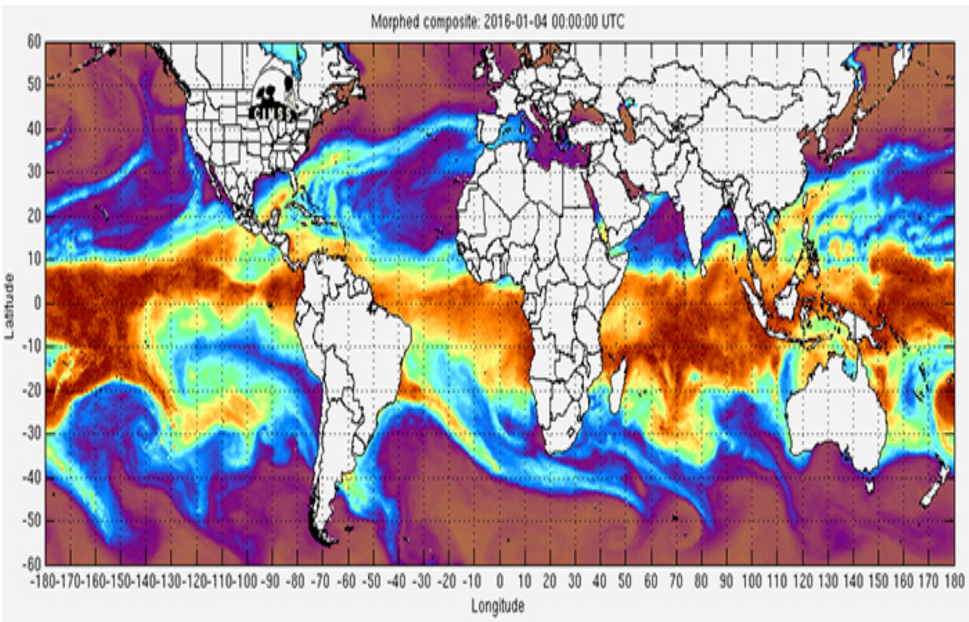

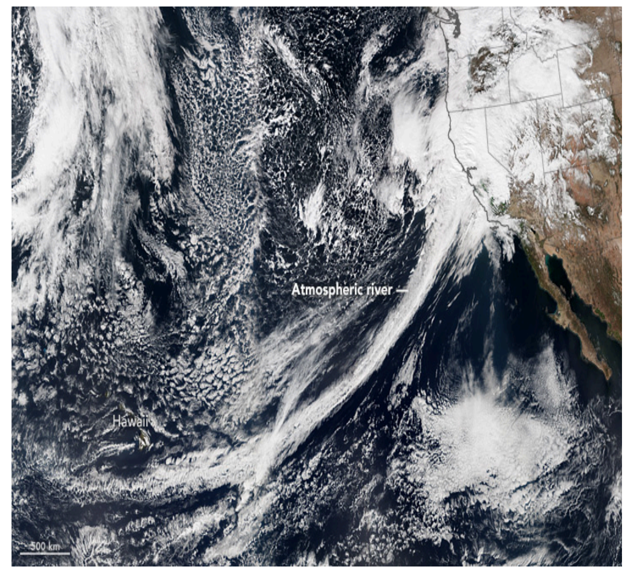

AR detection using Integrative water vapor transport (IVT) from MERRA2

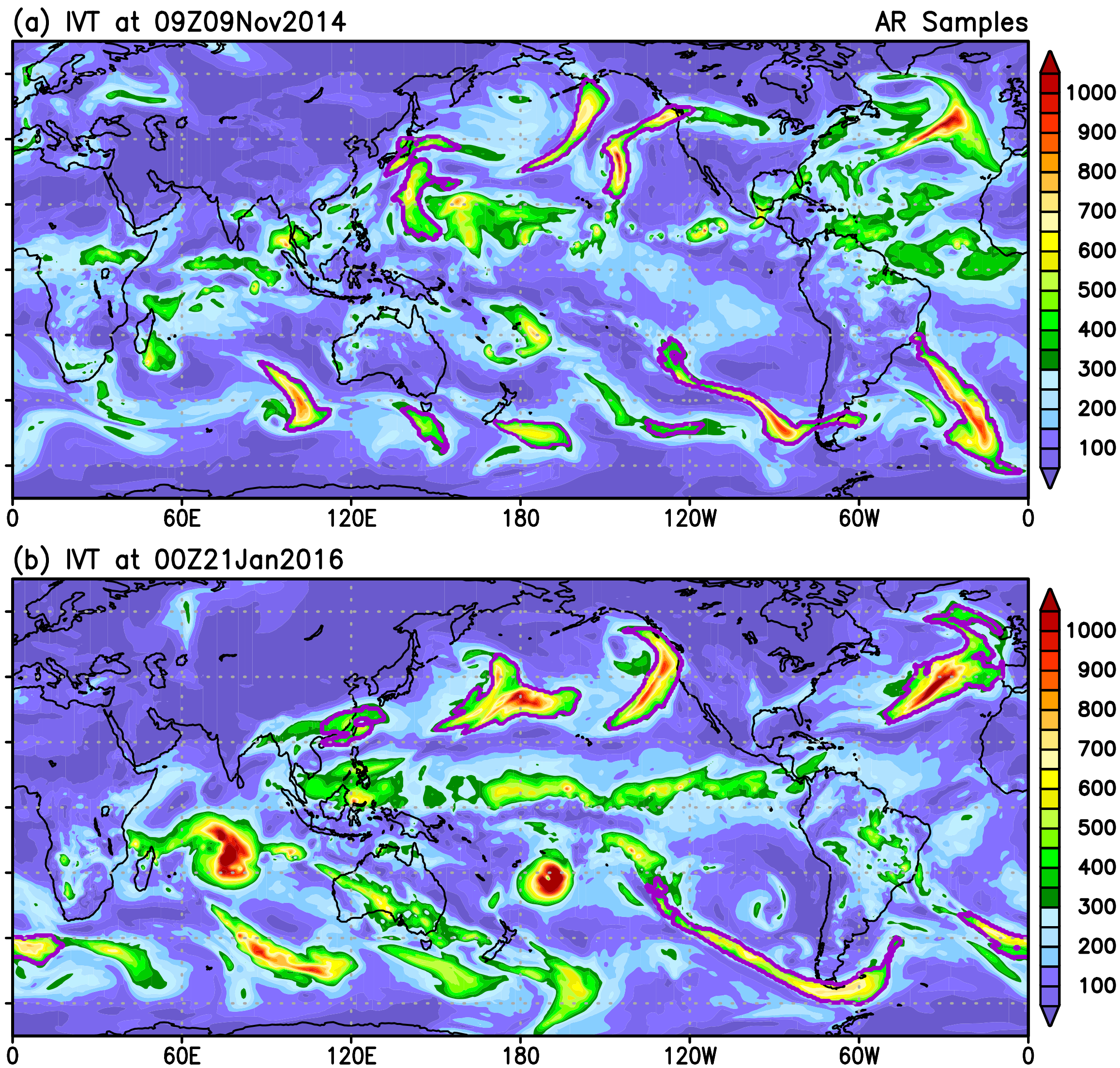

GPM CSH heating profiles (Tao et al., 2018)

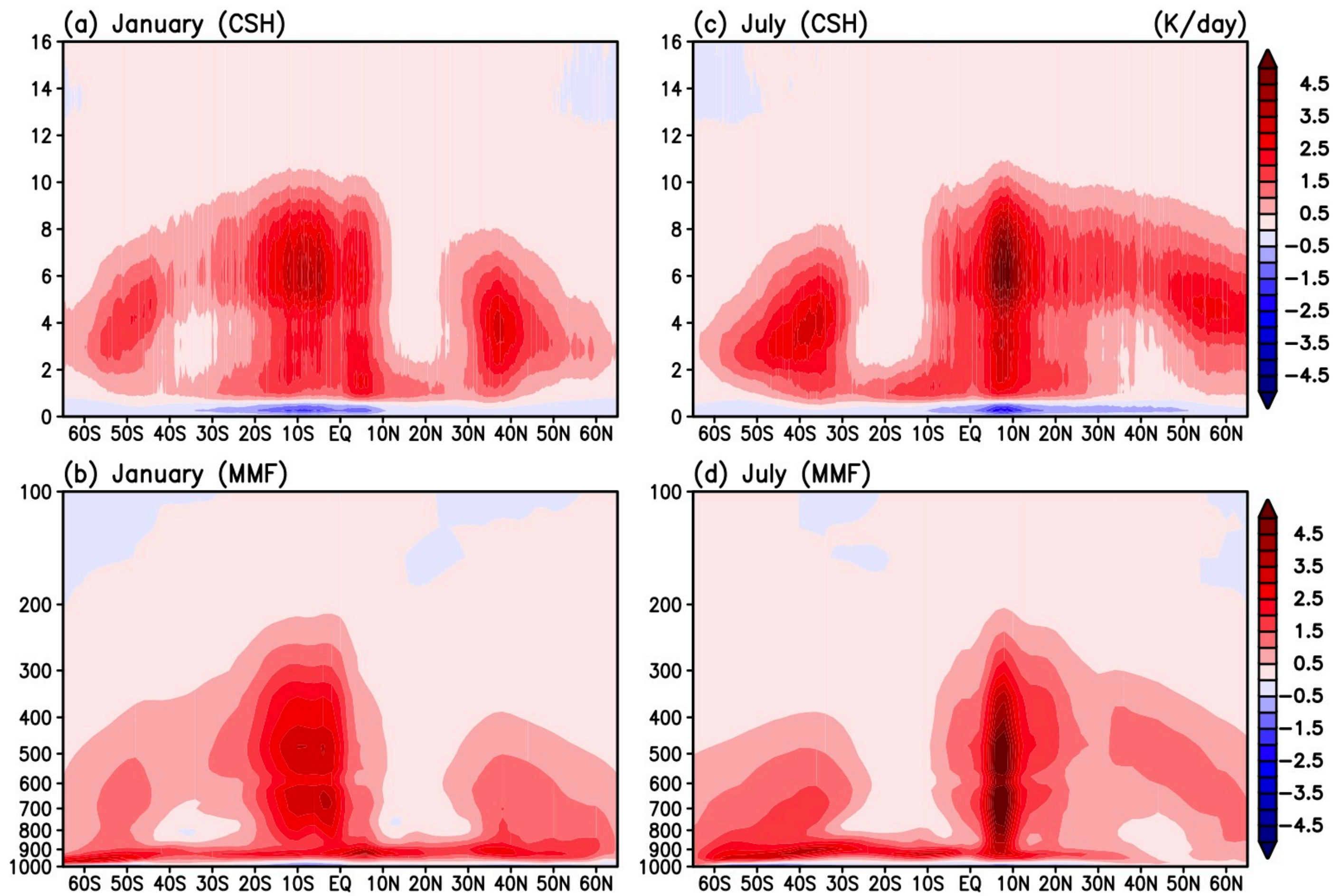

11

Stronger, deeper LH profiles over eastern N. Pacific and US westcoast during ARs

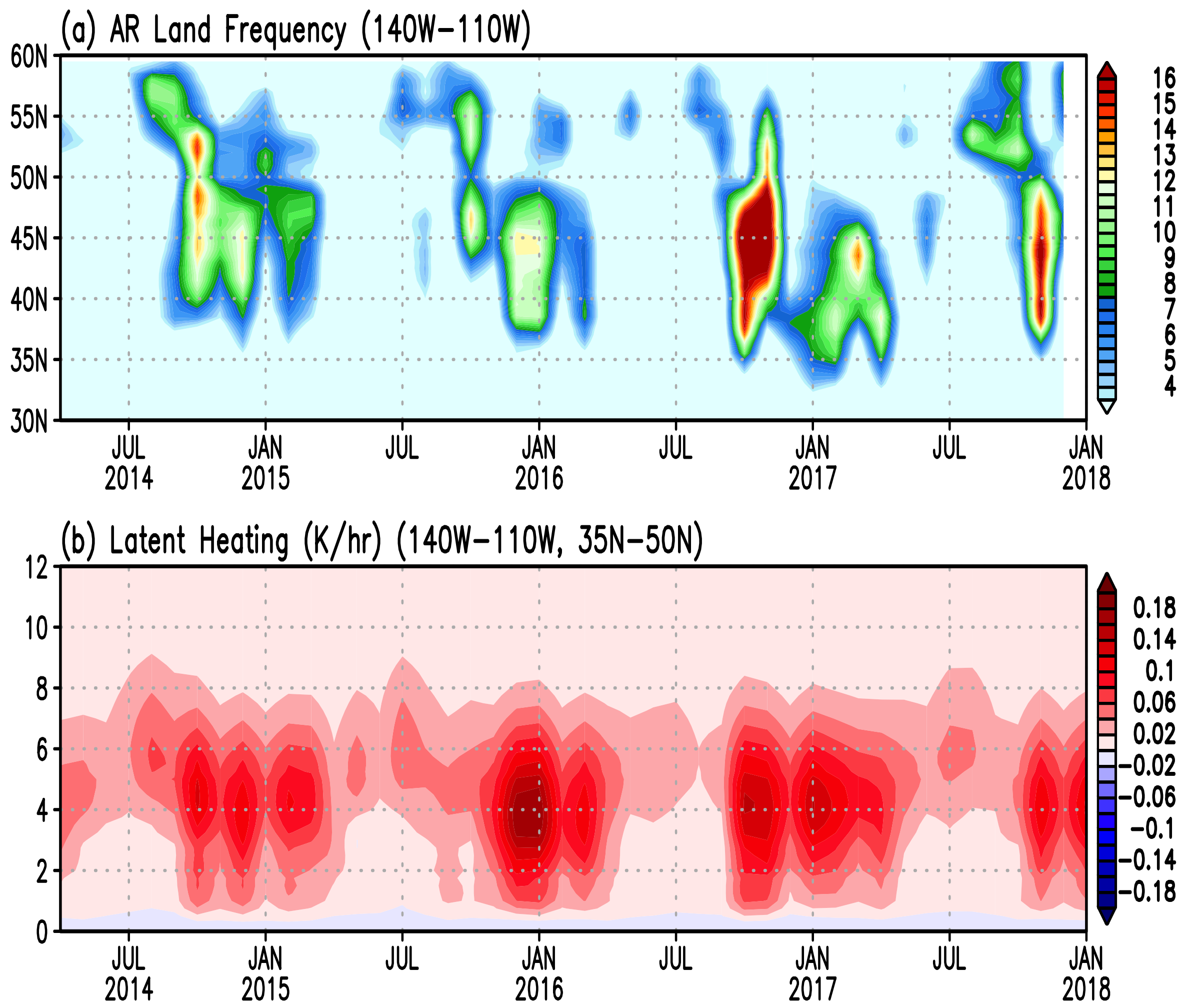

ITCZ convection and Atmospheric River

Active ARs

Inactive ARs

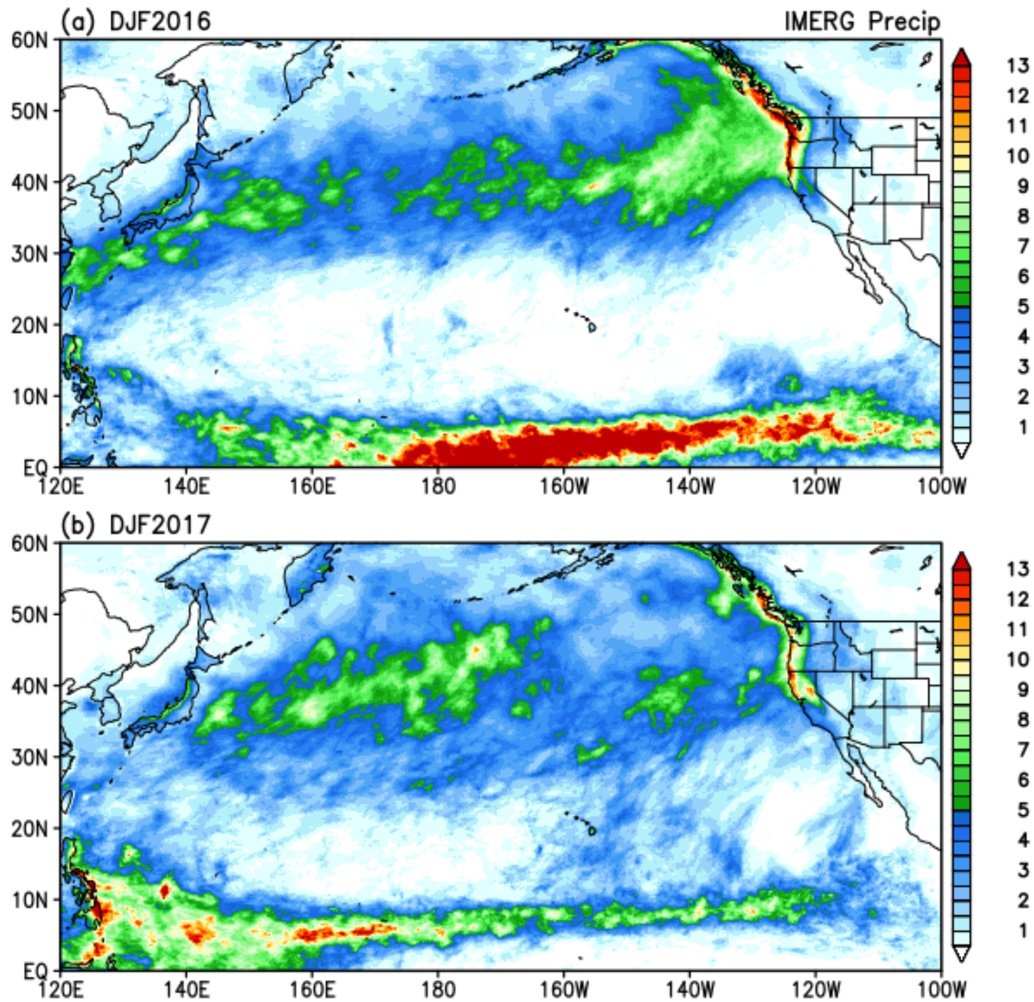

Enhanced Atmospheric River under DTS ?

AR frequency

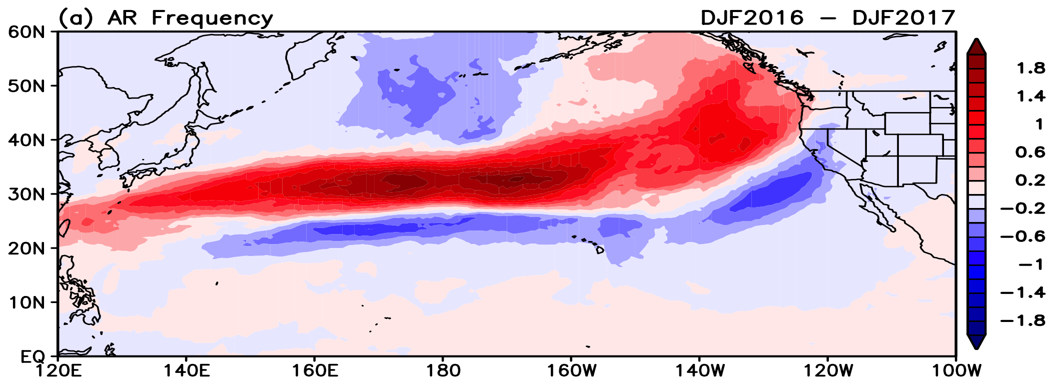

IMERG rainfall

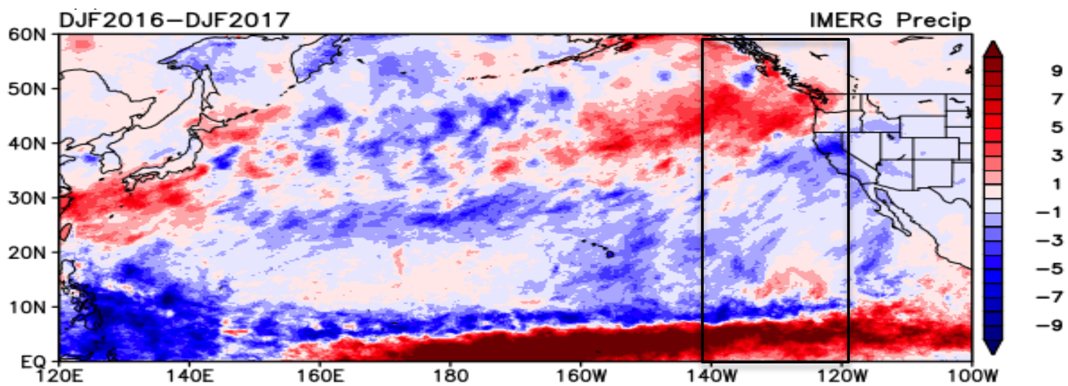

LH profile change

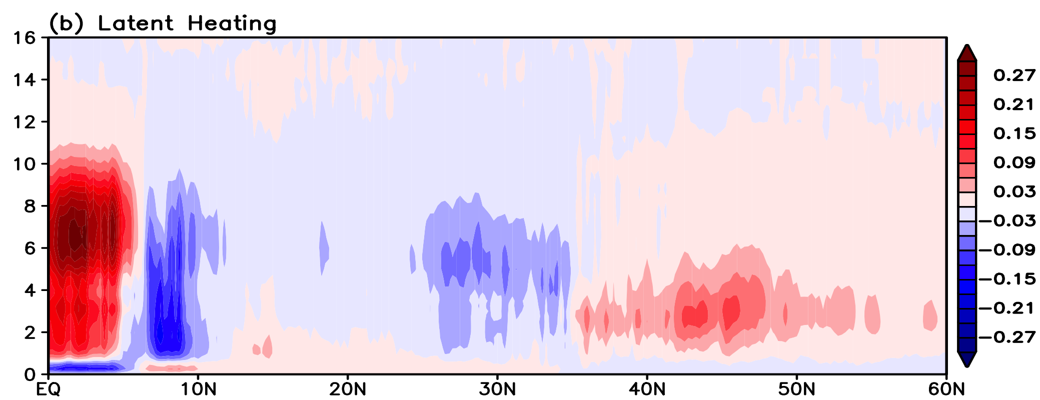

MODIS Cloud Regime (CR) Classification daily, global, 1x 1 degree (2000-2015)

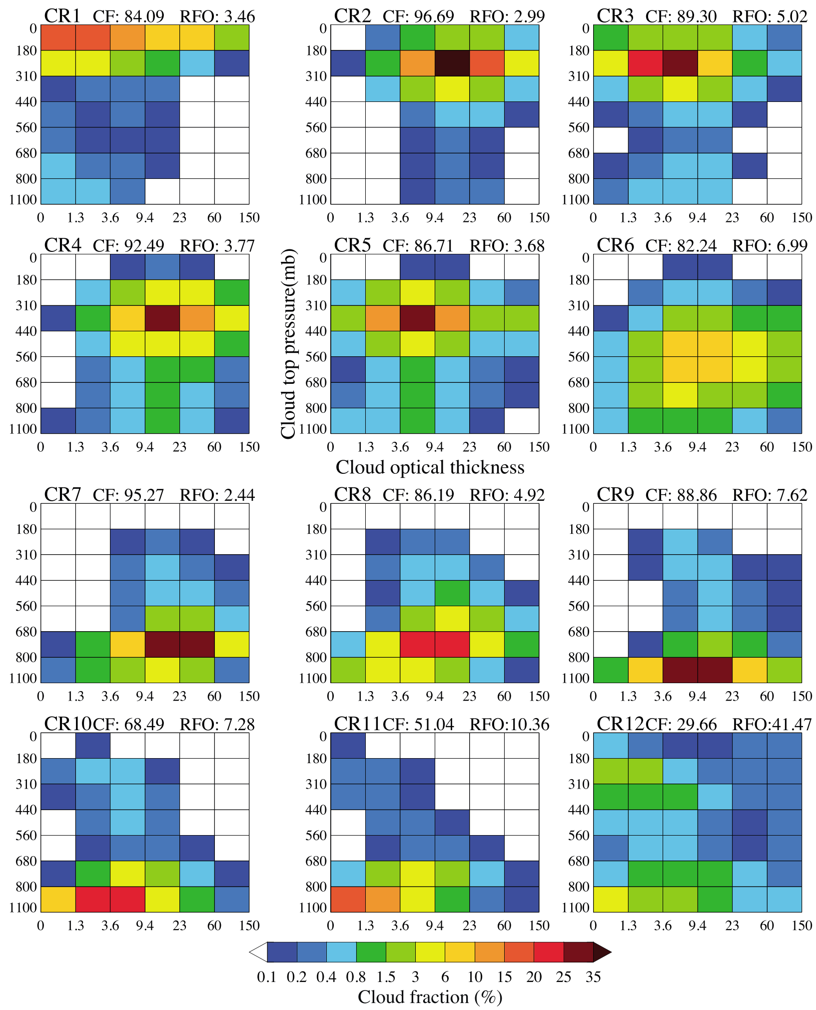

Figure 1. Centroids (mean histograms) of the 12 cloud regimes (CRs) derived from clustering analysis on 12 years of MODIS C6 Aqua-Terra p_c-τ joint daily histograms at a resolution of 1°. Additional information included in each panel is the mean global cloud fraction CF and relative frequency of occurrence (RFO) of each CR.

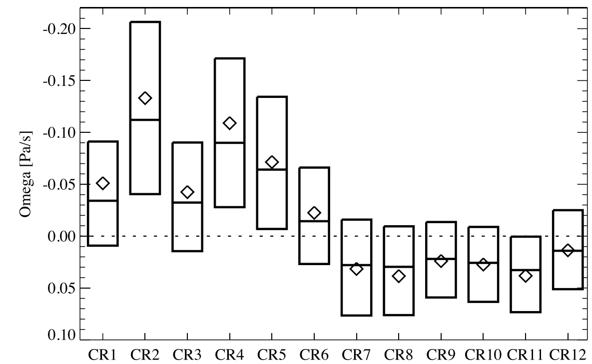

Figure 3. Boxplot of the 500 hPa large-scale vertical velocity associated with each CR, derived from compositing MERRA data. The box length indicates the interquartile range, the horizontal line is the median, and the symbol represents the mean.

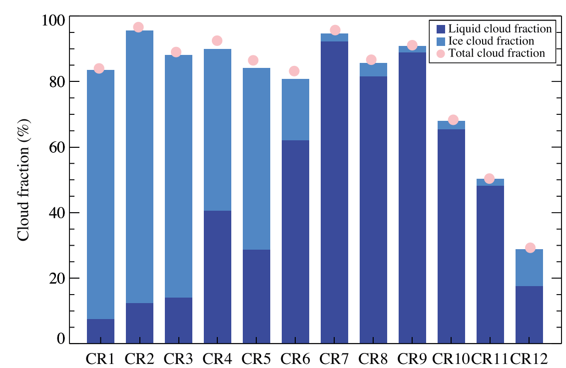

Figure 4. Liquid, ice, and total CF for each CR derived from compositing gridded MODIS A_c values. The total A_c values are slightly above the sum of liquid and ice A_c because of pixels of undetermined thermodynamic phase.

Oreopoulos et al (2016)

Cloud Regime analyses for AR

←-Deep cl

clouds-→

12 Cloud F

LWP..)

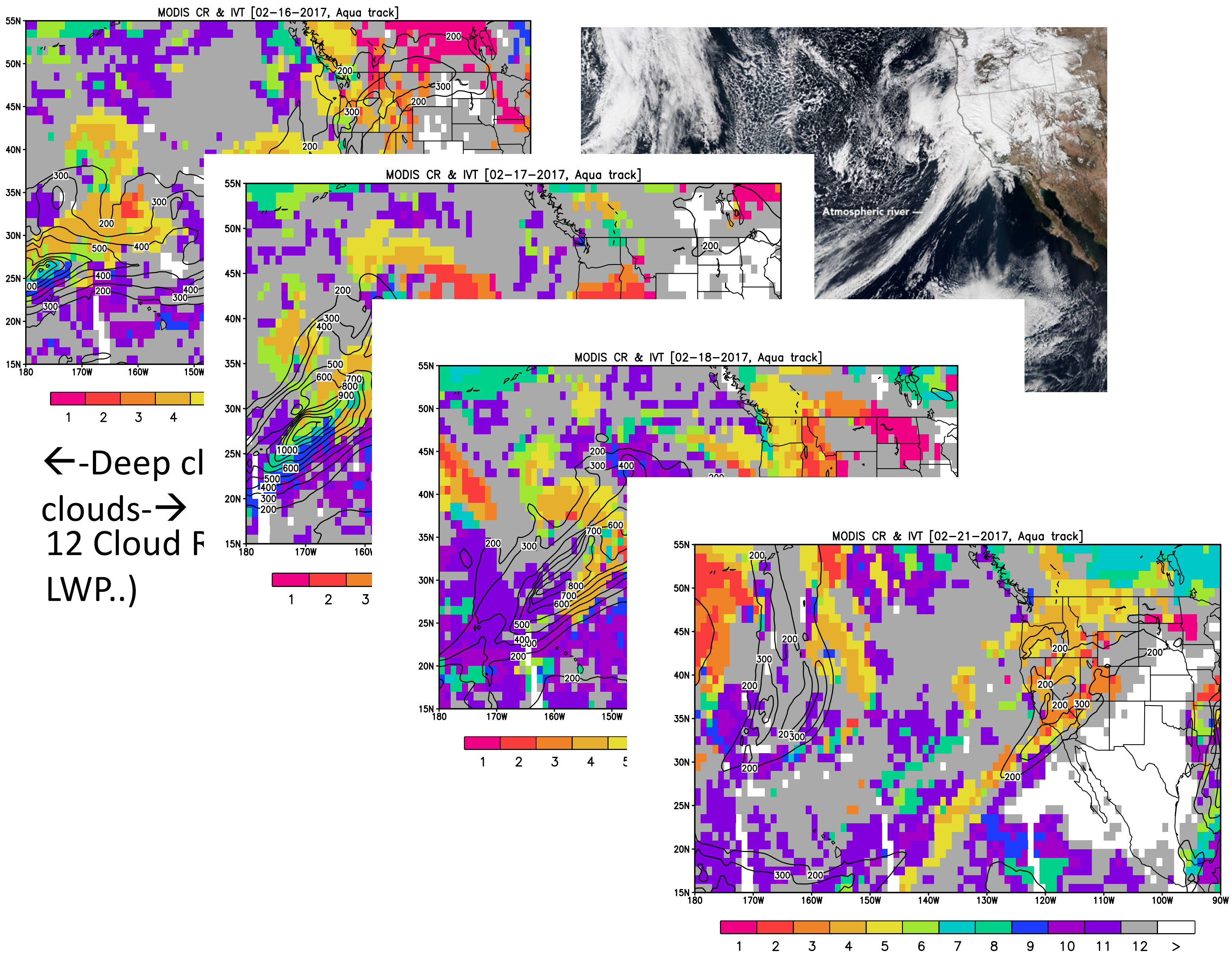

[140-110W, 35-50N]

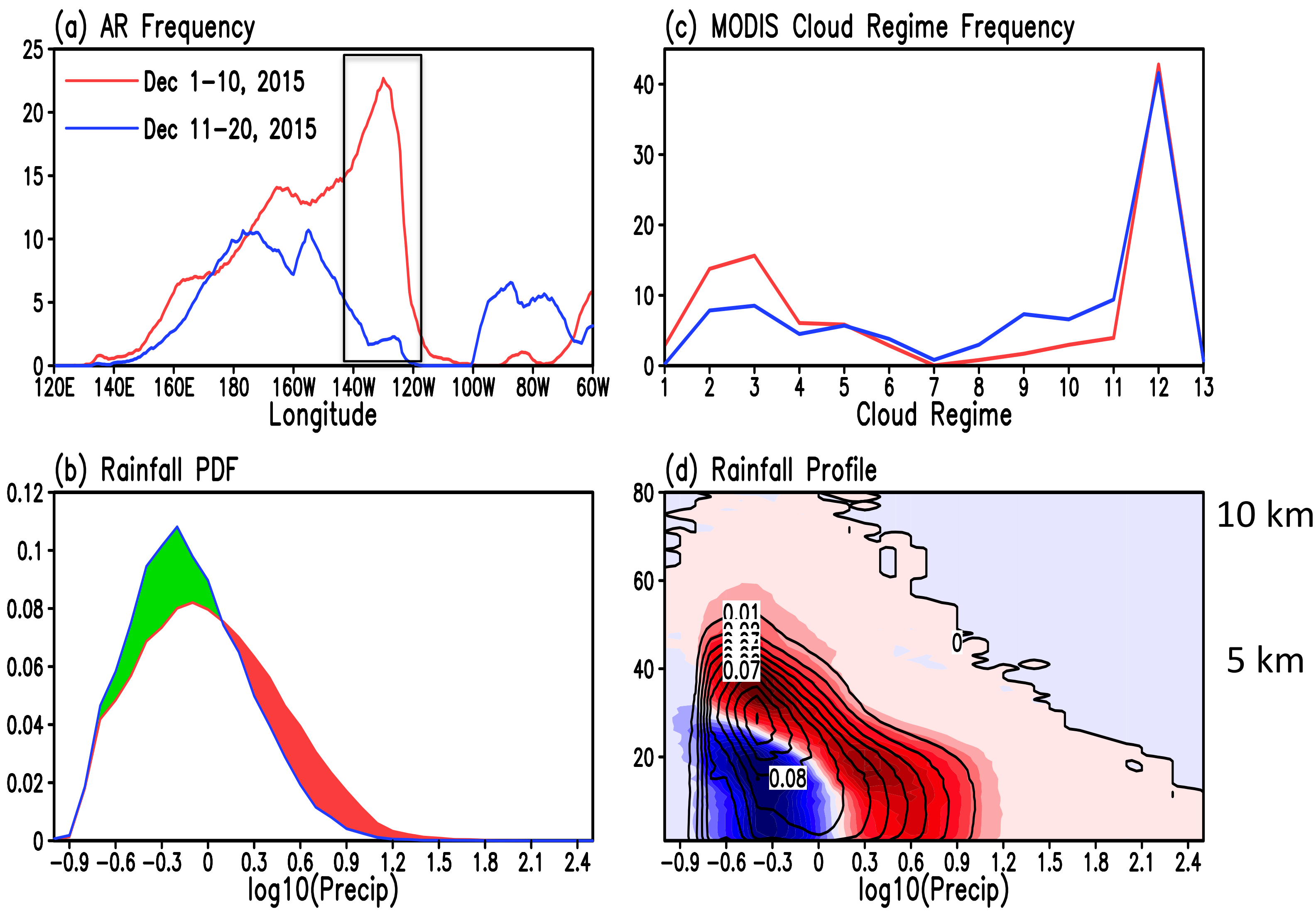

IMERG rainrate pdf

KU-band CFAD

The Deep Tropical Squeeze (DTS) Hypothesis : A testbed for cloud-radiation-circulation interactions

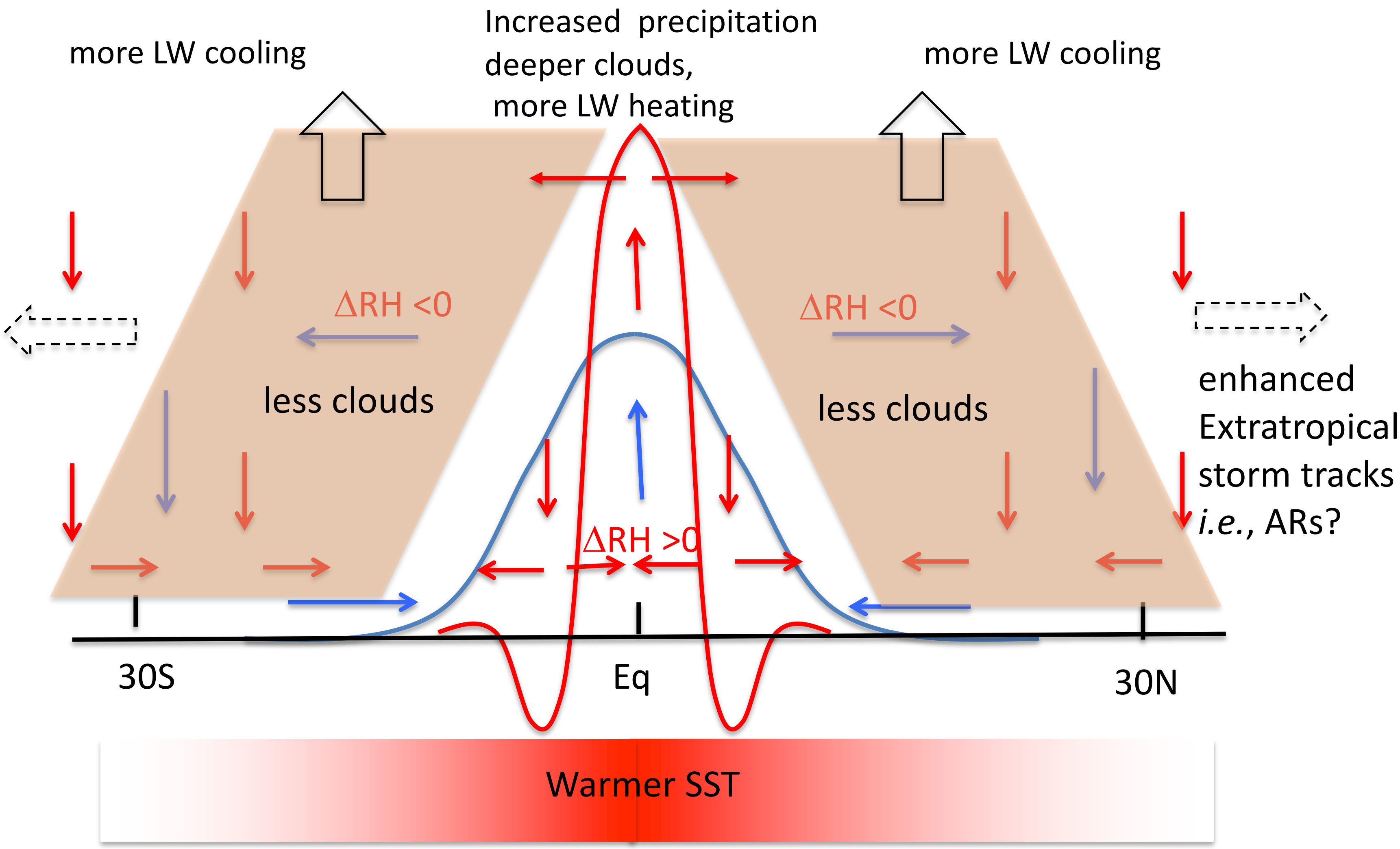

Back up Slides

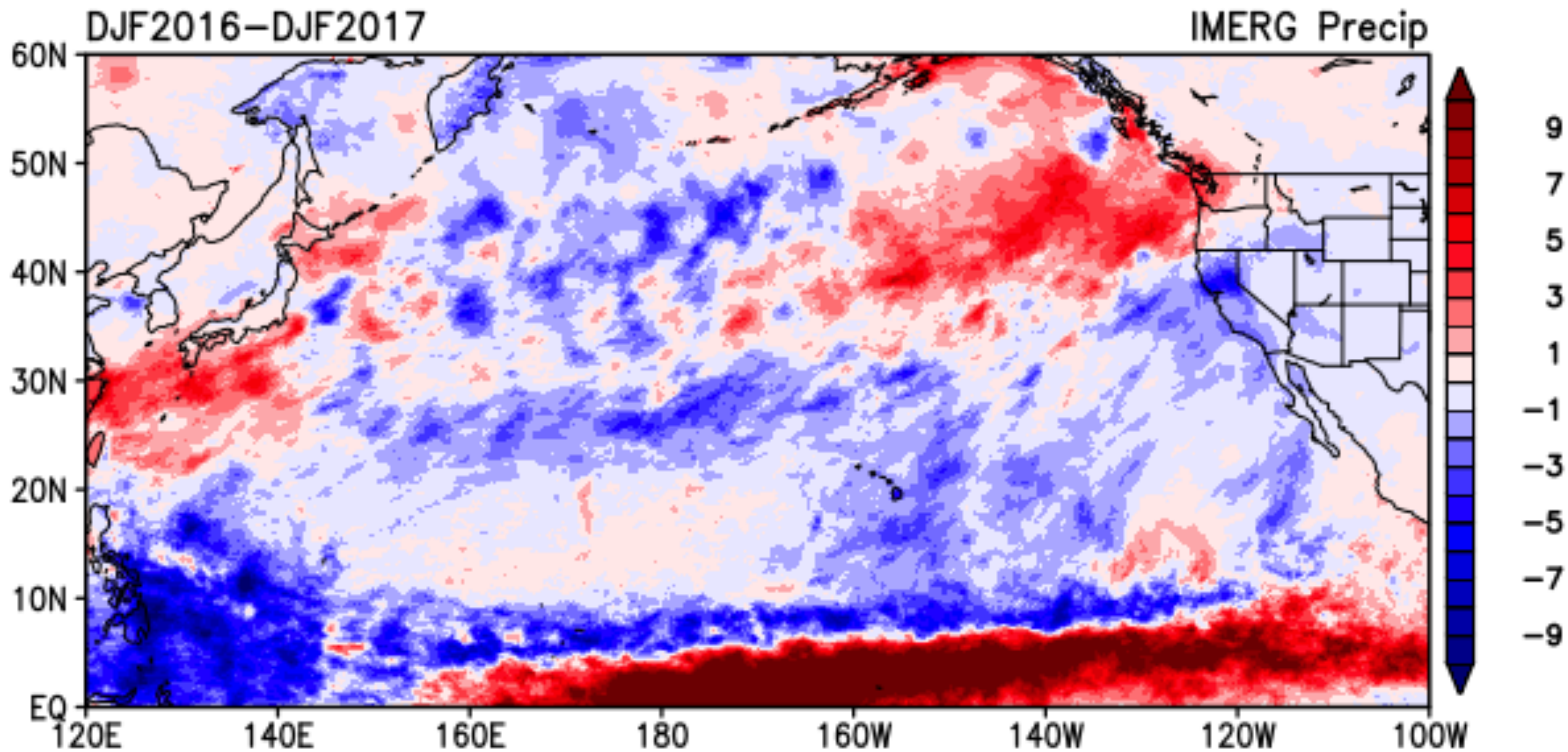
DJF2016–DJF2017
IMERG Precip
60N
50N
40N
30N
20N
10N
EQ
120E
140E
160E
180
160W
140W
120W
100W
9
7
5
3
1
−1
−3
−5
−7
−9

Cloud regime analysis for ARs

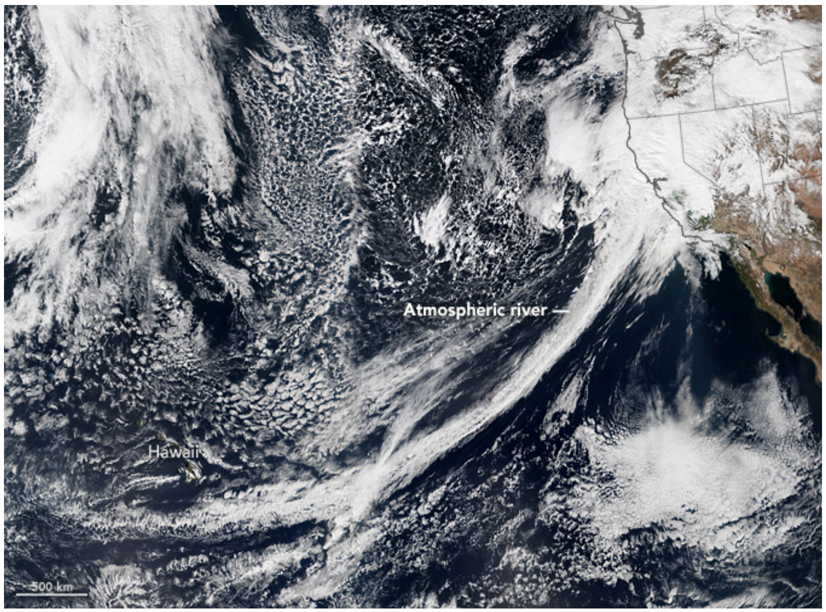

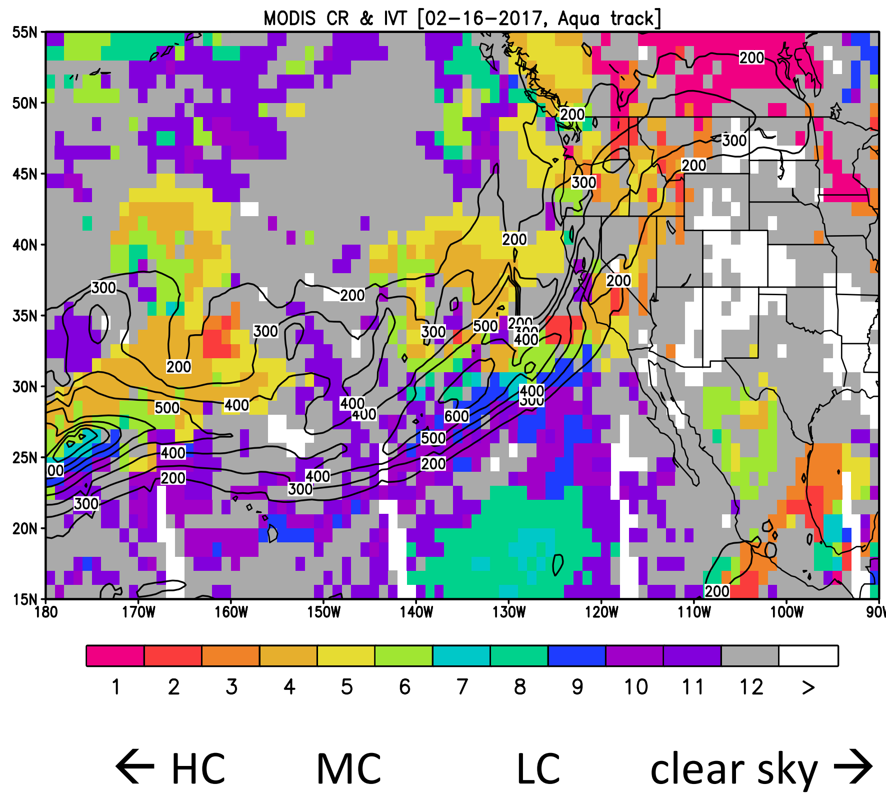

Modulation of AR activities and ITCZ convection by CRCI

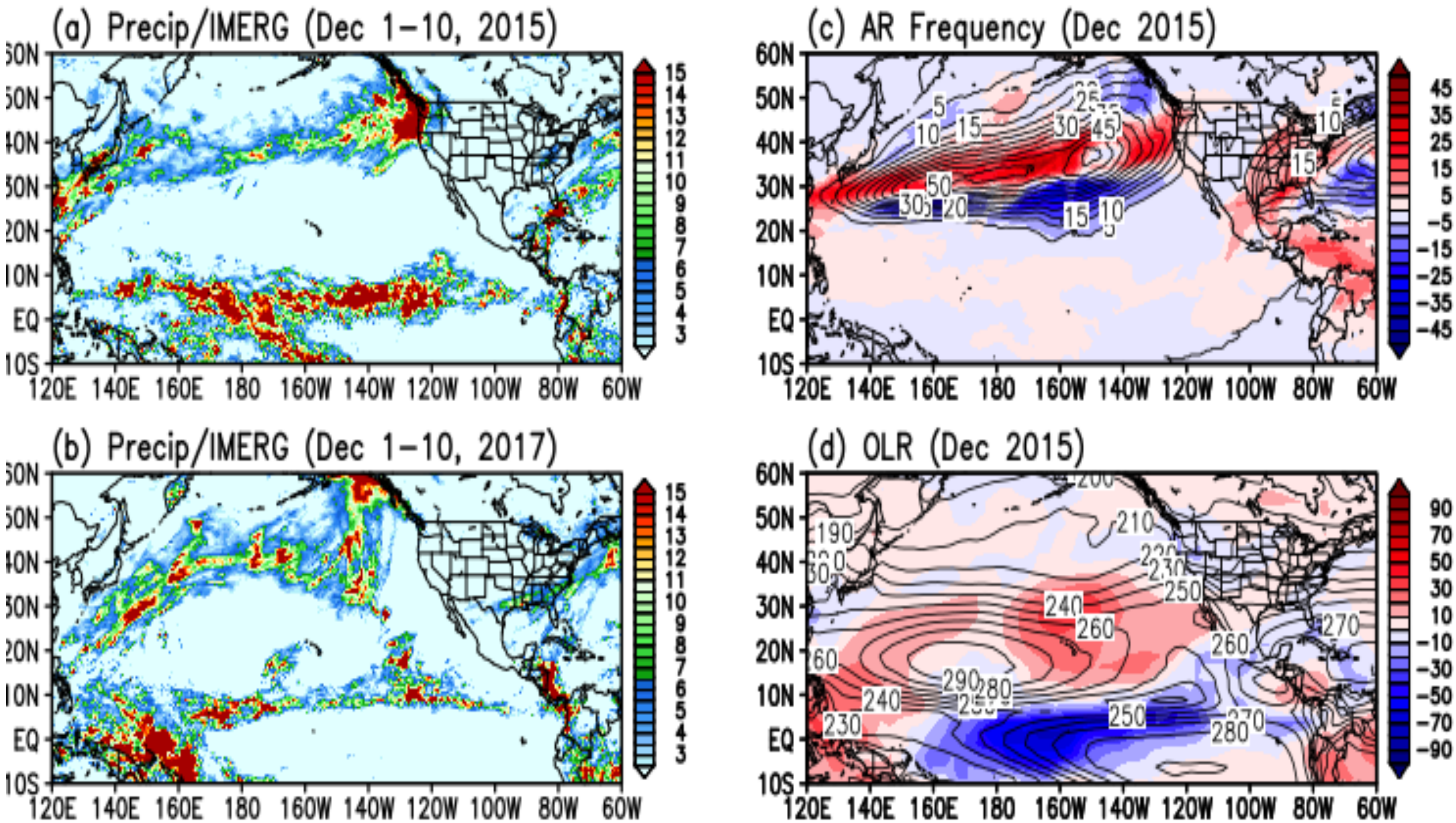

Back Up slides

Changes in diabatic heating and dynamical tendencies

$$\frac{\partial \bar{s}}{\partial t} + \overline{\boldsymbol{v}} \cdot \nabla \bar{s} + \bar{\omega}\frac{\partial \bar{s}}{\partial p} = Q_R + L(c-e) - \nabla \cdot \overline{s'v'} - \frac{\partial \overline{s'\omega'}}{\partial p}$$

$$\frac{\partial s}{\partial t} = DYN + Q_{MP} + Q_{SW} + Q_{LW} + Q_{Res} \sim 0, \qquad for\ steady\ state$$

where s= moist static energy (CpT + gz)

$DYN = -\left(\overline{\boldsymbol{v}} \cdot \nabla \bar{s} + \bar{\omega}\frac{\partial \bar{s}}{\partial p}\right)$, dynamical tendency

Q_{MP}, heating by moist physics

Q_{SW}, shortwave heating

Q_{LW}, longwave heating

Q_{res} transients, unresolved subgrid processes

- Fig. 9,

  Anomalies of CSH latent heating profile for strong vs. weak ITCZ rainfall

Plot TOA area-weighted radiative SW and LW fluxes climatologies and anomalies to Compare with vertical mass flux in same coordinates

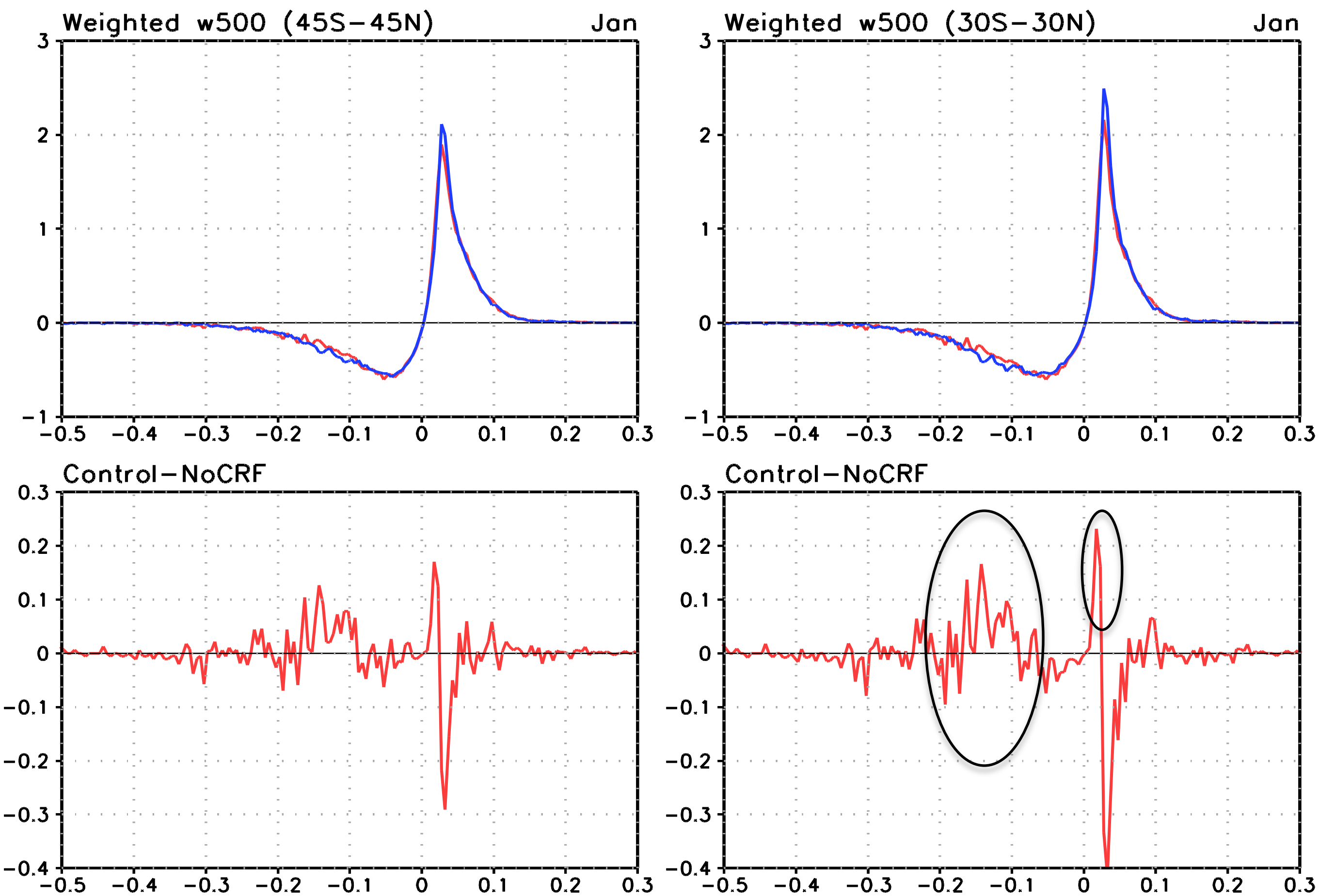

Find out out what are the geographic locations of points contributing to the the circled features.

Additional figures

Comparison of Q_{MP}, Q_{SW} and Q_{LW} from GMMF to:

Zonal mean radiative heating profile, from

Cloudsat HERB (L'Ecuyer et al. 2010 ??)

Fig. 2

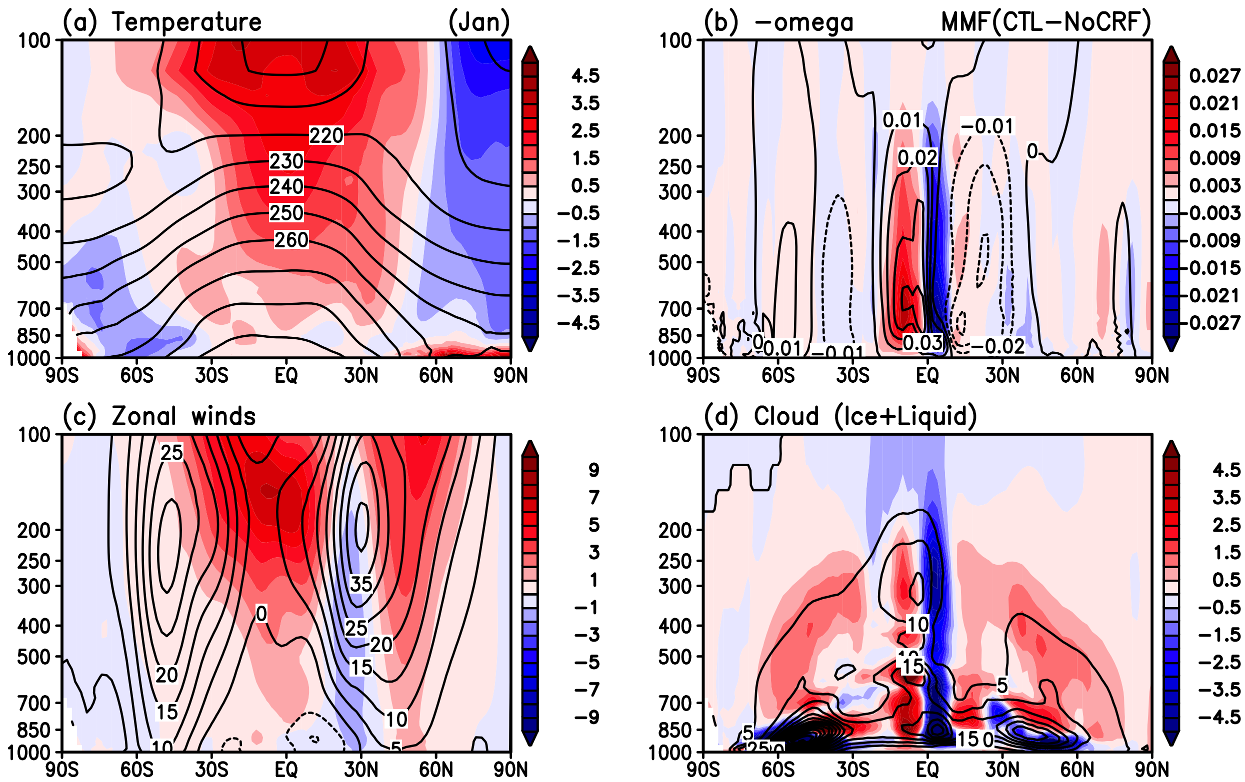

Change zonal wind to relative humidity

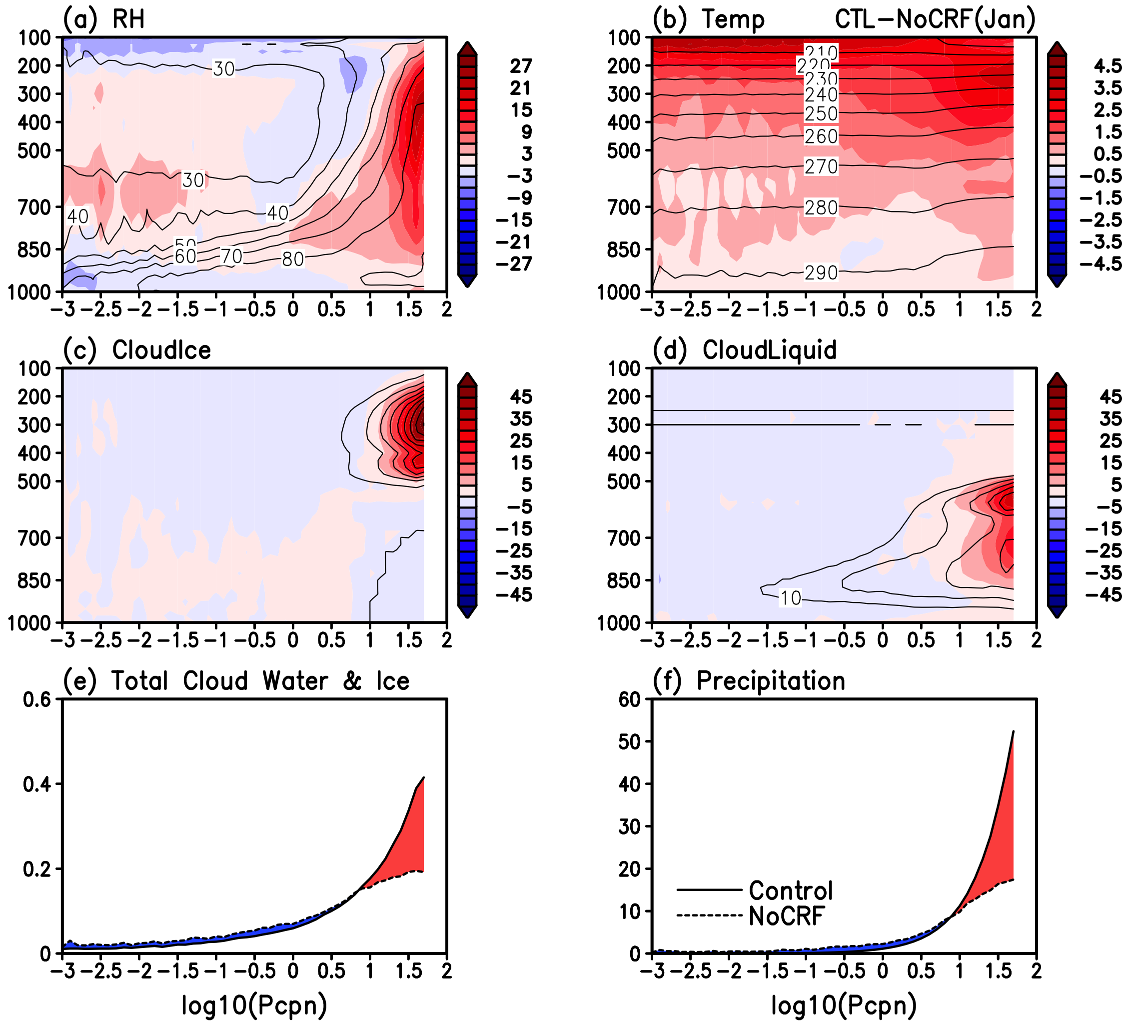
(a) RH
(b) Temp CTL−NoCRF(Jan)
(c) CloudIce
(d) CloudLiquid
(e) Total Cloud Water & Ice
(f) Precipitation
Control
NoCRF
log10(Pcpn)
log10(Pcpn)

Figure 7

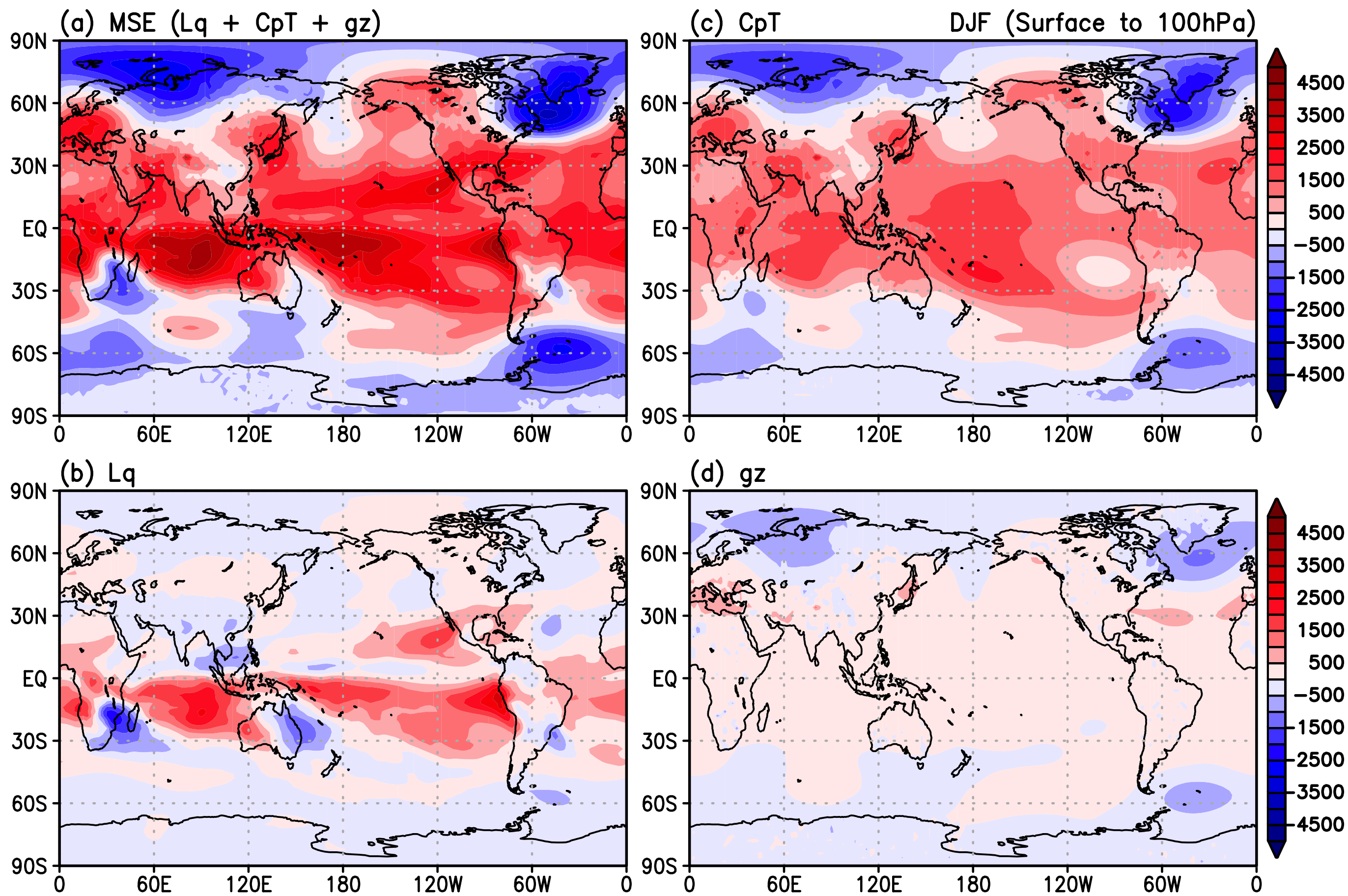

$$\left[\partial\bar{h}/\partial t\right] = -\left[\frac{\bar{\omega}\partial\bar{h}}{\partial p}\right] - \left[\bar{\boldsymbol{V}}\cdot\nabla\bar{h}\right] - \left[\frac{\overline{\omega'\partial h'}}{\partial p}\right] - \left[\overline{\boldsymbol{V}'\cdot\nabla \mathrm{h}'}\right] + SH + LH + [SW] + [LW]$$